J. Fluid Mech. (2005), *vol.* 533, *pp.* 183–192.
doi:10.1017/S002211200500443X Printed in the United Kingdom

Anomalous scaling of low-order structure functions of turbulent velocity

By S. Y. CHEN[1], B. DHRUVA[2], S. KURIEN[3], K. R. SREENIVASAN[4] AND M. A. TAYLOR[5]

[1]Department of Mechanical Engineering, Johns Hopkins University, Baltimore, MD 21218

[2]Schlumberger Cambridge Research, Madingley Road, Cambridge CB3 0EL

[3]Center for Nonlinear Studies (CNLS) and Mathematical Modeling & Analysis Group (T7), Los Alamos National Laboratory, Los Alamos, NM 87505

[4]International Centre for Theoretical Physics, Strada Costiera 11, 34014 Trieste, Italy

[5]Computer and Computational Sciences (CCS-3), Los Alamos National Laboratory, Los Alamos, NM 87505

(Received 3 November 2004 and in revised form 21 February 2005)

It is now believed that the scaling exponents of moments of velocity increments are anomalous, or that the departures from Kolmogorov's (1941) self-similar scaling increase nonlinearly with the increasing order of the moment. This appears to be true whether one considers velocity increments themselves or their absolute values. However, moments of order lower than 2 of the absolute values of velocity increments have not been investigated thoroughly for anomaly. Here, we discuss the importance of the scaling of non-integer moments of order between $+2$ and -1, and obtain them from direct numerical simulations at moderate Taylor microscale Reynolds numbers $R_\lambda \leqslant 450$, and experimental data at high Reynolds numbers ($R_\lambda \approx 10\,000$). The relative difference between the measured exponents and Kolmogorov's prediction increases as the moment order decreases towards -1, thus showing that the anomaly is manifested in low-order moments as well.

1. Introduction

The moments of velocity differences over spatial scales of size r, the so-called structure functions, provide useful measures of the statistical description of fluid turbulence (Kolmogorov 1941*a*, *b*). In particular, the longitudinal structure functions defined as

$$S_n(\boldsymbol{r}) = \langle [(\boldsymbol{u}(\boldsymbol{x}+\boldsymbol{r}) - \boldsymbol{u}(\boldsymbol{x}))\cdot\hat{\boldsymbol{r}}]^n \rangle \tag{1.1}$$

have been studied extensively. Here, $\boldsymbol{u}(\boldsymbol{x})$ is the velocity vector at position $\boldsymbol{x}$, and $\hat{\boldsymbol{r}}$ is the unit vector along the separation vector $\boldsymbol{r}$. The special interest in structure functions comes in part from an exact result, known as the 4/5 law,

$$S_3(\boldsymbol{r}) = -\tfrac{4}{5}\epsilon r, \tag{1.2}$$

valid in the inertial range of scales ($\eta \ll r \ll L$ where η is the Kolmogorov scale characterizing the dissipative scale of motion and L is a suitable large scale of turbulence); ϵ is the mean rate of energy dissipation. In part, the interest is spurred by the operational ease with which longitudinal structure functions can be obtained from experimental data if one makes the so-called Taylor's hypothesis (Taylor 1935). The major impetus for measurements, however, is the scaling result of Kolmogorov – K41

for brevity – that, for high Reynolds numbers, the structure functions follow the relation $S_n(\boldsymbol{r}) \sim r^{\zeta_n}$ where the scaling exponent $\zeta_n = n/3$. As a result of considerable work over forty years (see, for example, Anselmet *et al.* 1984; Maurer Tabeling & Zocchi 1994; Arneodo *et al.* 1996; Sreenivasan & Antonia 1997), it now appears nearly certain that the scaling exponents deviate from $n/3$ increasingly and nonlinearly as n increases. This is the anomalous scaling. While some issues remain to be explained satisfactorily (see, for example, Sreenivasan & Dhruva 1998), it appears that anomalous scaling is a genuine result worthy of a serious theoretical effort. Consequently, there has been considerable research directed to this problem (e.g. L'vov & Procaccia 1996).

One obvious property of high-order moments is that they sample the tails of the probability distribution function (PDF) of velocity increments. Since some of the associated rare events may be related to well-defined flow structures in real space, which in turn may be affected by shear and other non-universal effects, it is not entirely certain that the results for high-order moments are universal. In contrast, low-order moments are determined nearly entirely by the core of the PDF, and the relative effects of rare events, among which may be non-universal shear effects, are thus diminished. Thus, it is reasonable to regard anomalous scaling – and its universality – as more conclusively established if low-order moments also display anomaly. This is the subject of this paper.

The lowest non-trivial structure function that has been studied extensively is the second order, whose scaling exponent has been shown to be ≈ 0.7. Though this is measurably different from the predicted value of 2/3, the difference is too small to be conclusive on its own. It would thus be useful to examine scaling exponents for moments of still lower orders. Assuming that the probability p for zero-valued velocity increments is finite, that is, $p((\boldsymbol{u}(\boldsymbol{x}+\boldsymbol{r})-\boldsymbol{u}(\boldsymbol{x}))\cdot\hat{\boldsymbol{r}}=0)>0$ for each $\boldsymbol{r}$, moments of order -1 and below do not exist (see also Castaing, Gagne & Hopfinger 1990). Therefore, the range of our current interest is limited to $-1 < n \leqslant 2$, where n is necessarily fractional. With decreasing n in this range, if the deviation from $n/3$ decreases, we shall at least know that K41 will be exact in the limit of low-order moments, and regard it as a possible reference point for a theory. If, on the other hand, these deviations remain non-trivial, it may well be that the understanding of the anomaly can be sought more fruitfully in terms of low-order moments, for the simple reason that such a theory can justifiably ignore rare events (which, as previously mentioned, may also be non-universal). Some preliminary measurements were published in Sreenivasan *et al.* (1996), Cao, Chen & Sreenivasan (1996) and Kurien & Sreenivasan (2001*b*), but the present paper is a more complete account of the data and the analysis. More importantly, the preliminary numbers did not take account of the possible effects of residual anisotropy in both experiments and simulations, an issue whose importance has been highlighted recently (e.g. Biferale & Procaccia 2004). We take account of this feature using a recently developed angle-averaging technique (Taylor, Kurien & Eyink 2003) and consider their new simulations data at Taylor microscale Reynolds number, R_λ, of 450.

2. Experimental and numerical data

2.1. *High-Reynolds-number atmospheric boundary layer measurements*

Hot-wire measurements were made in the atmospheric surface layer at a height of 35 m above the ground using a standard meteorological tower at Brookhaven National Laboratory. The tower itself presented very little obstacle to the wind because of its low solidity. The dataset analysed here is part of a more comprehensive batch obtained

U	u'	ϵ	η	λ	R_λ
$7.6\,\mathrm{m\,s^{-1}}$	$1.36\,\mathrm{m\,s^{-1}}$	$0.032\,\mathrm{m^2\,s^{-3}}$	0.57 mm	11.4 mm	10 340

TABLE 1. Some relevant parameters for the atmospheric data. Here, U is the mean speed, u' is the root-mean-square velocity, ϵ is the mean rate of energy dissipation, η and λ are the Kolmogorov and Taylor microscales, respectively, and $R_\lambda \equiv u'\lambda/\nu$, ν being the kinematic viscosity of air at the measurement temperature.

at the tower. The hot wire, 0.7 mm in length and 0.5 μm in diameter, was placed facing the wind, about 2 m from the tower. (For monitoring the wind direction, the tower was equipped with a vane anemometer placed 2 m from the measurement station.) The calibration was performed *in situ* using a TSI calibrator and checked later in a wind tunnel. The signals were low-pass filtered at 5 kHz and sampled at 10 kHz. The anemometer and signal conditioners were placed nearby at the height of measurement, and the conditioned signal was transmitted to the ground and digitized using a 12-bit A/D converter. Typical data records contained between 10 and 40 million samples, during which time the wind direction and its mean speed were deemed acceptably constant. More details are given in Dhruva (2000), but the essential features for this particular set of data are listed in table 1. The wind conditions were somewhat unstable.

2.2. *Direct numerical simulations (DNS) of Navier–Stokes equations with forcing*

The Navier–Stokes equations were solved numerically for periodic boundary conditions. A pseudospectral code was used using a second-order time-integration scheme (Cao *et al.* 1996). Simulations were carried out with a resolution of 512^3 grid points on the CM-5 at Los Alamos National Laboratory and SP machines at IBM Watson Research Center. To obtain a statistically steady state, a forcing is applied to the first wavenumber shells $0.5 < k < 1.5$ so that at each time step the total energy of that shell is constant. This procedure does not fix the energy of the individual modes or their phases. Comparisons between these simulations and data from other simulations with different forcing schemes are satisfactory (see, for example, Wang *et al.* 1996). The maximum R_λ was about 250. Time integration up to 60 large-eddy turnover times was performed.

Even though the 512^3 data show a well-developed scaling range in an ESS (extended self-similarity) plot, the Reynolds number is not large enough to produce unambiguous scaling in direct log-log plots of moments versus the scale r. It was also found that, even though the turbulence is nominally isotropic, there are some measurable (though small) differences between the scaling of longitudinal and transverse structure functions, suggesting a possible presence of residual anisotropy in the inertial range, arising from possible anisotropy in forcing. For these two reasons, it seemed worth considering new data from a higher Reynolds number simulation, for which the anisotropy effects, to the extent that they were present at all, were accounted for in a rational manner. We therefore used the velocity data from a simulation of the Navier–Stokes equation in a periodic domain of size 1024^3. The forcing scheme, described in Taylor *et al.* (2003), is similar in some respects to that for the 512^3 simulation but the primary difference is that the forced modes are free to oscillate in amplitude as well. The steady state was achieved in about 1.5 large-eddy turnover times and the simulation ran for a total of 2.5 large-eddy turnover times. The statistical analysis was performed over 10 frames in the final eddy turnover time. The steady state value of R_λ was 450. Other parameters of this simulation are given in table 2.

N	ν	ϵ	$\delta x/\eta$	R_λ
1024	3.5×10^{-5}	1.75	0.75	450

TABLE 2. Some relevant parameters for the 1024^3 DNS. The fourth column provides the resolution of the simulation in terms of the Kolmogorov scale.

Order of moments	Measured exponents	Relative difference	DNS exponents (512^3)	Relative difference	DNS exponents (1024^3)	Relative difference
−0.80	−0.317	0.189	−0.313	0.174	-	-
−0.60	–	–	–	–	-0.238 ± 0.002	0.188
−0.40	–	–	–	–	-0.158 ± 0.001	0.181
−0.20	−0.078	0.170	−0.077	0.155	-0.078 ± 0.001	0.171
0.10	0.039	0.170	0.036	0.080	0.039 ± 0.001	0.155
0.20	0.076	0.140	0.073	0.095	0.077 ± 0.001	0.152
0.30	0.113	0.130	0.112	0.120	0.115 ± 0.001	0.147
0.40	0.150	0.125	0.150	0.125	0.152 ± 0.001	0.143
0.50	0.187 ± 0.003	0.140	0.187	0.122	0.190 ± 0.001	0.138
0.60	0.221	0.105	0.223	0.115	0.226 ± 0.001	0.133
0.70	0.265	0.136	0.260	0.114	0.263 ± 0.001	0.128
0.80	0.292	0.095	0.296	0.110	0.300 ± 0.001	0.123
0.90	0.333	0.110	0.332	0.107	0.340 ± 0.001	0.119
1	0.372	0.116	0.366	0.098	0.370 ± 0.006	0.111
1.25	0.458	0.099	0.452	0.085	0.459 ± 0.006	0.101
1.50	0.542	0.084	0.536	0.072	0.545 ± 0.006	0.091
1.75	0.628	0.077	0.619	0.061	0.630 ± 0.006	0.079
2.00	0.704 ± 0.003	0.061	0.699	0.049	0.712 ± 0.006	0.064

TABLE 3. Scaling exponents from ESS compared with those for isotropic turbulence from two sets of DNS data. Error bars are given for the experimental data for two exponents. Those for the 512^3 data are given in Cao *et al.* 1996. Columns 3, 5 and 7 list the relative differences from the K41 prediction, $(\zeta_n - n/3)/(n/3)$, of the exponents calculated using different schemes.

3. Results

Since we are interested in real-valued structure functions, we can consider, when the moment order is either fractional or negative, only the moments of absolute values of velocity differences defined as

$$S_{|n|}(\boldsymbol{r}) = \langle |(\boldsymbol{u}(\boldsymbol{x}+\boldsymbol{r}) - \boldsymbol{u}(\boldsymbol{x})) \cdot \hat{\boldsymbol{r}}|^n \rangle. \tag{3.1}$$

In experimental measurements, because the Reynolds number is quite high (see table 1), and the scaling ranges reasonably clear, we have the luxury of estimating the scaling exponent directly from log-log plots of $S_{|n|}(\boldsymbol{r})$ versus r (see Dhruva 2000).

We also performed the calculation using ESS (Benzi *et al.* 1993). In ESS, a structure function $S_n(\boldsymbol{r})$ of interest is plotted against another structure function $S_m(\boldsymbol{r})$ and the relative scaling exponent ζ_n/ζ_m is obtained. In particular, if the exponent of $S_m(\boldsymbol{r})$ is known *a priori*, as from theory for the third-order structure function (see (1.2)), then the exponent of $S_n(\boldsymbol{r})$ may be inferred. It is known that ESS improves the scaling range significantly. In the present case we use $S_m(\boldsymbol{r}) = S_{|3|}(\boldsymbol{r})$, the absolute third-order structure function and assume its scaling exponent is 1. It is unclear if this assumption is valid since the K41 theory does not apply to moments of absolute differences; indeed, it appears that the scaling exponents of S_3 and $S_{|3|}$ are slightly different (Sreenivasan *et al.* 1996). However, we found that the ESS exponents (see table 3) were

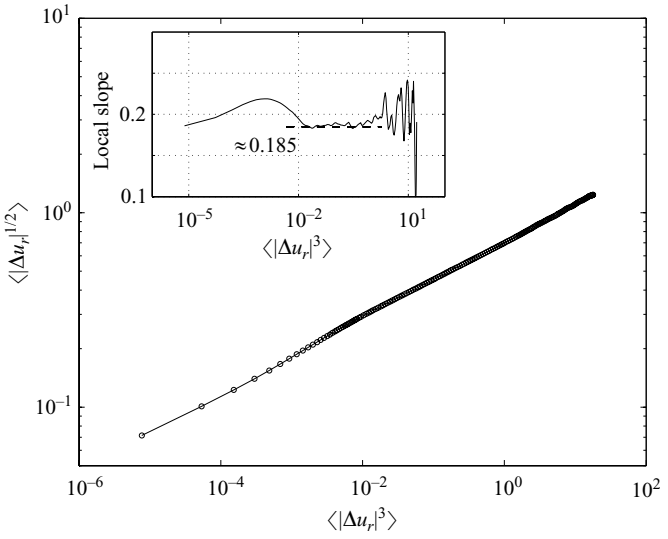

FIGURE 1. ESS calculation of scaling exponent of order 0.5 from experimental data.

within the uncertainty of those obtained directly by Dhruva (2000). An example of ESS plot for moment-order of 0.5 is shown in figure 1, along with the local slope (see inset).

For the numerical simulation data with resolution of 512^3, the exponents were obtained only by ESS because the scaling region was small in direct log-log plots against the scale r. These exponents are listed in table 3. The table also lists $(\zeta_{|n|} - n/3)/(n/3)$, the relative departures from the K41 prediction, for each scheme used to calculate the exponents.

3.1. *Effects of finite Reynolds number and anisotropy*

The finite Reynolds number of turbulence in numerical work shortens the inertial range over which scaling exponents may be discerned with clarity. This remains a constraint because the applicable theory concerns the limit of $Re \to \infty$. A constraint in experimental data is that some large-scale anisotropy might be present in the range that appears to scale. The effect could be present even in high-Reynolds-number flows because the effects of anisotropic forcing penetrate the scaling range in a subtle but systematic way; see, for example, Arad, L'vov & Procaccia (1999*b*), Kurien & Sreenivasan (2000, 2001*a*). In numerical simulations, the statistics are usually calculated with the separation direction $\hat{\boldsymbol{r}}$ oriented parallel to a box-side. If there is residual anisotropy (angular-dependence) in the small-scales, this procedure will bias the results. Since we are concerned here with delicate results, this uncertainty has to be eliminated satisfactorily.

3.2. *Recovering isotropic statistics by angle averaging*

We make use of two recent developments to properly eliminate the effect of anisotropy in the inertial range of the 1024^3 data. First, we now know that isotropic and anisotropic contributions can be isolated systematically by projecting structure function of a given order over a particular basis function in its SO(3) group decomposition (e.g. Arad *et al.* 1998, 1999*a*; Kurien *et al.* 2000; Biferale & Procaccia 2004). This is a useful step to take even in nominally isotropic turbulence because the effect of forcing might persist in the nominal scaling range. Second, Taylor *et al.* (2003) developed a method by which the third-order longitudinal structure function

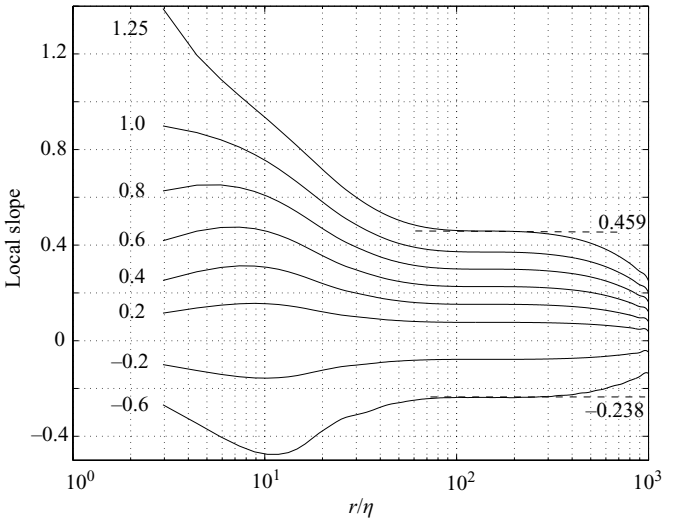

FIGURE 2. The scaling exponents, equal to the local slopes $\zeta_{|n|} = \mathrm{d}\log(S_{|n|}(r))/\mathrm{d}\log(r)$, as a function of r, for various values of $-1 < n < 2$ for the 1024^3 DNS data. Each curve is labelled by the order of the structure function. The scaling exponents deduced in this way are given on the right for two representative orders, $n = 1.25$ and -0.6. For comments on the behaviour for very small r, see text.

was computed in many directions of the flow for a given r and the results averaged. The angle-averaged value of the structure function achieved the Kolmogorov 4/5 prediction to a remarkable degree, thus providing a convincing scheme for extracting the isotropic component of a mildly anisotropic flow. The two procedures achieve the same goal: the angle-averaging procedure is in effect a projection on to the isotropic component of the SO(3) rotation group. Since this method is independent of the order of the structure function, we use it as described below for fractional statistics.

The angle-averaged isotropic structure function in the computational domain D is given by

$$S_{|n|}(r) = \frac{1}{\Delta t}\int_{t_0}^{t_0+\Delta t} \mathrm{d}t \int \frac{\mathrm{d}\Omega_r}{4\pi} \int_D \frac{\mathrm{d}\boldsymbol{x}}{L^3}\, |(\boldsymbol{u}(\boldsymbol{x}+\boldsymbol{r}) - \boldsymbol{u}(\boldsymbol{x}))\cdot\hat{\boldsymbol{r}}|^n, \tag{3.2}$$

where the usual average for a particular direction of the unit separation vector $\hat{\boldsymbol{r}}$ is followed by a spherical average of all possible orientations of $\hat{\boldsymbol{r}}$ over the solid angle Ω_r. The long-time average is taken in the steady state. In units of the large-eddy turnover time, t_0 is 1.5 from the start of the simulation and Δt is unity.

In numerical simulations, since we have the full three-dimensional velocity field, we can in principle integrate over the sphere and project out the isotropic part of $S_{|n|}$. Taylor *et al.* showed that the full spherical average may be approximated to arbitrary precision by first computing the structure function over sufficiently many different directions in the flow, interpolating each of these functions by a simple single-variable cubic spline, and then averaging the interpolated values over all directions. This angle averaging of the structure functions is much faster to implement than interpolating the three-dimensional, three-component velocity data over spherical shells in order to perform the integration.

However, angle averaging comes at a price: as with all interpolation procedures, it introduces errors at the very smallest scales. This is evident in figure 2 where the local

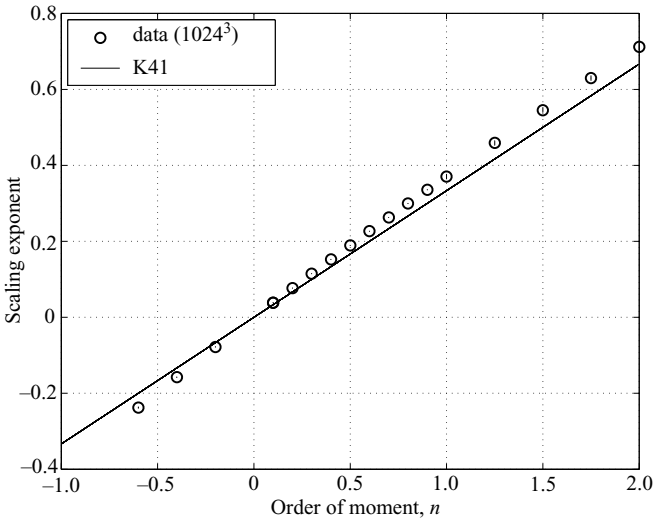

FIGURE 3. The scaling exponents calculated from the 1024^3 DNS (○); standard deviations ($\approx \pm 0.001$) are smaller than the size of the circles. Full line: K41 exponents, extrapolated via self-similarity arguments to low-order statistics. Anomalous scaling is evident.

slopes do not asymptote as expected from the Taylor expansion for $r \to 0$. We have verified that this error does not propagate to values of r in the scaling region. Angle averaging does not alter the scaling exponents observed in figure 2 but marginally extends the range for large r.

The angle-averaging procedure was performed for all orders. For very low-order moments $|n| < 1$ we observed only marginal anisotropy in the inertial range and the statistics computed in the different directions nearly coincided with each other except for large scales $r/\eta > 300$. In figure 2 we show the logarithmic derivative (the local slope) of the structure functions for various fractional orders. If the local slope is constant over a range of r, it provides the scaling exponent $\zeta_{|n|}$. A rough estimate of the inertial range from figure 2 is $50 < r/\eta < 140$ and the error estimate on the scaling exponent is calculated as the variance over this range. As expected, the smaller the absolute order $|n|$, the more constant is the local slope, thus indicating that our confidence level improves as the moment order decreases. The scaling exponents and their uncertainty over the inertial range are given for a range of fractional orders in table 3, column 6. The exponents calculated for all three datasets display a good degree of agreement.

The scaling exponents computed in this way from the 1024^3 simulation are plotted as a function of order n in figure 3. For comparison, the K41 exponents are also shown. The measured exponents deviate from the K41 values essentially for all orders. This shows that the intermittency, until now thought to be characteristic of only high-order moments, sampling 'fat' tails of the PDF of velocity increments, persists into the low-order moments sampling the core of the PDF. Figure 4 shows the difference $(\zeta_{|n|} - n/3)$ from the K41 prediction as a function of n. There is a linear approach to zero with a slope of 0.056. Equivalently, the behaviour near zero is $\zeta_{|n|} = 0.38n$ instead of $\zeta_{|n|} = n/3$.

Figure 5 shows that the relative departure of the measured scaling exponents from the self-similarity prediction of K41, $(\zeta_{|n|} - n/3)/(n/3)$, is a smooth function of n in the range $-1 < n \leqslant 10$. We also present for comparison the anomalous exponents

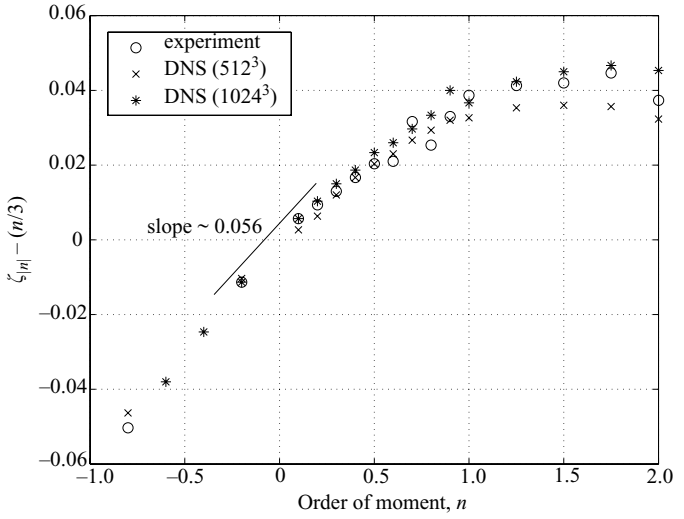

FIGURE 4. The departure from K41 for all three data sets: experiment (○), 512^3 DNS (×) and 1024^3 DNS (★). The difference goes to zero approximately linearly with a slope of ~ 0.056. This indicates that the departure from K41 persists even in the vicinity of $n = 0$. See figure 5 for the relative departure from K41.

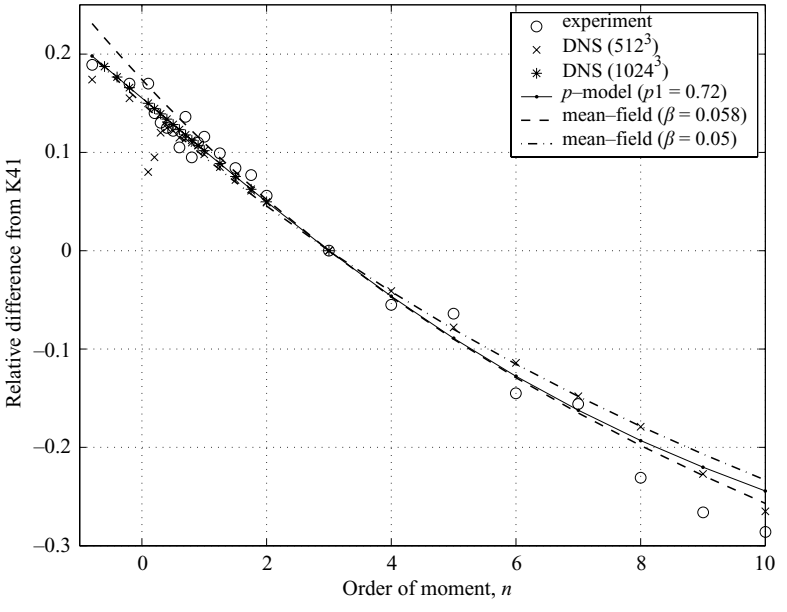

FIGURE 5. The relative difference $(\zeta_{|n|} - n/3)/(n/3)$ for the various $-1 < n \leqslant 10$ as calculated from the experiments (○), DNS (512^3) (×) and DNS (1024^3) (★). The exponents for $n > 3$ for the experiments and the 512^3 simulation are taken from the values tabulated in Dhruva (2000). The solid line represents the outcome of the p-model (Meneveau & Sreenivasan 1987) for $p = 0.72$. The dashed and dotted lines are the predictions from the dynamical theory of Yakhot (2001), with two slightly different values of the parameter β in the theory.

calculated from the multifractal p-model (Meneveau & Sreenivasan 1987) and the dynamical theory of Yakhot (2001) for two values of the parameter β in the theory. (Yakhot (2001) inferred $\beta = 0.05$ and Kurien & Sreenivasan (2001*b*) inferred 0.058.)

The dependence on n in the range $-1 < n \leqslant 3$ is more or less linear and becomes weakly quadratic for $n > 3$. The exact 4/5 result of K41 with scaling exponent 1 takes the relative difference to zero at $n = 3$. A noteworthy point is $n = 0$. This relative difference goes smoothly through $n = 0$ without any special feature, showing that while the measured exponents also go to zero at $n = 0$, they do so at a different rate than the K41 exponents (see figures 3 and 4). That is, there is a finite departure from K41 of $\sim$ 15% for $n \to 0$. There is also no special behaviour as $n \to -1$ at which point the mathematically defined scaling exponent, and hence the relative difference from K41, diverges.

4. Discussion and conclusions

The principal result of this paper is that the fractional low-order moments have scaling exponents that are different from $n/3$. In this sense, it is reasonable to consider that anomaly exists in low-order and negative moments up to -1. Thus, instead of focusing entirely on high-order moments in search of an explanation for intermittency, it may also be reasonable to attempt to understand anomaly in low-order moments. This has the advantage that rare events, whose universality may be in some doubt, play far less of a role.

The present analysis may be recast in terms of the probability distribution function of velocity increments. The prediction according to self-similarity is that $p(\Delta u(r) = 0, r) \sim r^{-1/3}$, that is the probability distribution function for zero-valued velocity increments should scale as $r^{-1/3}$. Departures from this scaling would indicate departures from self-similarity for small values of the velocity increment. Previous results using the same experimental data (Kurien & Sreenivasan 2001*b*) have shown that there is measurable departure from $r^{-1/3}$ scaling of PDF for zero-valued velocity increments.

We close with a subtle remark. To keep structure functions real-valued for fractional orders, we can consider, in the range $-1 < n \leqslant 2$, only absolute valued velocity increments defined through (3.1). The difference between the classical structure functions defined in (1.1) and the corresponding ones defined for absolute-valued velocity increments is not completely clear. Our unpublished work appears to indicate that the absolute-valued structure functions have a larger scaling exponent than the classical ones when n is large and odd. It is thus possible, in principle, that the anomaly for small and fractional n may not be related very precisely to the anomaly observed for classical structure functions of high order.

We thank Victor Yakhot and Mark Nelkin for their valuable comments. S. K. acknowledges support from the DOE Office of Science Advanced Computing Research program in Applied Mathematics Research.

REFERENCES

Anselmet, F., Gagne, F., Hopfinger, E. J. & Antonia, R. A. 1984 High-order velocity structure functions in turbulent shear flow. *J. Fluid Mech.* **140**, 63–89.

Arad, I., Biferale, L., Mazitelli, I. & Procaccia, I. 1999*a* Disentangling scaling properties in anisotropic and inhomogeneous turbulence. *Phys. Rev. Lett.* **82**, 5040–5043.

Arad, I., Dhruva, B., Kurien, S., L'vov, V. S., Procaccia, I. & Sreenivasan, K. R. 1998 Extraction of anisotropic contributions in turbulent flows. *Phys. Rev. Lett.* **81**, 5330–5333.

Arad, I., L'vov, V. S. & Procaccia, I. 1999*b* Correlation functions in isotropic and anisotropic turbulence: The role of the symmetry group. *Phys. Rev.* E **59**, 6753–6765.

Arneodo, A., Baudet, C., Belin, F. *et al.* 1996 Structure functions in turbulence, in various flow configurations, at Reynolds number between 30 and 5000, using extended self-similarity. *Europhys. Lett.* **34**, 411–416.

Benzi, R., Ciliberto, S., Tripiccione, R., Baudet, C., Massaioli, F. & Succi, S. 1993 Extended self-similarity in turbulent flows. *Phys. Rev.* E **49**, R29–R32.

Biferale, L. & Procaccia, I. 2004 Anisotropy in turbulent flows and in turbulent transport. Submitted to *Phys. Rep.*; also at arXiv.org: nlin.CD/0404014.

Cao, N., Chen, S. & Sreenivasan, K. R. 1996 Scaling of low-order structure functions in homogeneous turbulence. *Phys. Rev. Lett.* **77**, 3799–3802.

Castaing, B., Gagne, Y. & Hopfinger, E. J. 1990 Velocity probability density-functions of high Reynolds-number turbulence. *Physica* D **46**, 177–200.

Dhruva, B. 2000 An experimental study of high-Reynolds-number turbulence in the atmosphere. PhD thesis, Yale University.

Kolmogorov, A. N. 1941*a* The local structure of turbulence in incompressible viscous fluid for very large Reynolds numbers. *Dokl. Akad. Nauk. SSR* **30**. Reproduced in *Proc. R. Soc. Lond.* A **434**, 9–13.

Kolmogorov, A. N. 1941*b* Dissipation of energy in the locally isotropic turbulence. *Dokl. Akad. Nauk. SSR* **32**, 16–18. Reproduced in *Proc. R. Soc. Lond.* A 1991 **434**, 15–17.

Kurien, S., L'vov, V. S., Procaccia, I. & Sreenivasan, K. R. 2000 Scaling structure of the velocity statistics in atmospheric boundary layers. *Phys. Rev.* E **61**, 407–421.

Kurien, S. & Sreenivasan, K. R. 2000 Anisotropic scaling contributions to high-order structure functions in high-Reynolds-number turbulence. *Phys. Rev.* E **62**, 2206–2212.

Kurien, S. & Sreenivasan, K. R. 2001*a* Measures of anisotropy and the universal properties of turbulence. In *New Trends in Turbulence, Les Houches Summer School 2000 Proceedings* (ed. M. Lesieur, A. Yaglom & F. David), pp. 55–111.

Kurien, S. & Sreenivasan, K. R. 2001*b* Dynamical equations for high-order structure functions, and a comparison of a mean-field theory with experiments in three-dimensional turbulence *Phys. Rev.* E **64**, 056302-16.

L'vov, V. & Procaccia, I. 1996 Turbulence: a universal problem. *Phys. World* **9**, 35–40.

Maurer, J., Tabeling, P. & Zocchi, G. 1994 Statistics of turbulence between two counterrotating disks in low-temperature helium gas. *Europhys. Lett.* **26**, 31–36.

Meneveau, C. & Sreenivasan, K. R. 1987 A simple multifractal cascade model for fully developed turbulence. *Phys. Rev. Lett.* **59**, 1424–1427.

Sreenivasan, K. R. & Antonia, R. A. 1997 The phenomenology of small-scale turbulence. *Annu. Rev. Fluid Mech.* **29**, 435–472.

Sreenivasan, K. R. & Dhruva, B. 1998 Is there scaling in high-Reynolds-number turbulence? *Prog. Theor. Phys. Suppl.* **130**, 103–120.

Sreenivasan, K. R., Vainshtein, S. I., Bhiladvala, R., San Gil, I., Chen, S. & Cao, N. 1996 Asymmetry of velocity increments in fully developed turbulence and the scaling of low-order moments. *Phys. Rev. Lett.* **77**, 8–11.

Taylor, G. I. 1935 Statistical theory of turbulence. I-IV *Proc. R. Soc. Lond.* A **151**, 421–478.

Taylor, M. A., Kurien, S. & Eyink, G. L. 2003 Recovering isotropic statistics in turbulence simulations: The Kolmogorov 4/5-th law *Phys. Rev.* E **68**, 26310-18.

Wang, L. P., Chen, S. Y., Brasseur, J. G. & Wyngaard, J. C. 1996 Examination of hypotheses in the Kolmogorov refined turbulence theory through high-resolution simulations. Part 1. Velocity field. *J. Fluid Mech.* **309**, 113–156.

Yakhot, V. 2001 Mean-held approximation and a small parameter in turbulence theory. *Phys. Rev.* E **63**, 026307-18.